

# SBS 0846+513: a new $\gamma$ -ray-emitting narrow-line Seyfert 1 galaxy

F. D'Ammando,<sup>1,2,3\*</sup> M. Orienti,<sup>2,4</sup> J. Finke,<sup>5</sup> C. M. Raiteri,<sup>6</sup> E. Angelakis,<sup>7</sup>  
L. Fuhrmann,<sup>7</sup> M. Giroletti,<sup>2</sup> T. Hovatta,<sup>8</sup> W. Max-Moerbeck,<sup>8</sup> J. S. Perkins,<sup>9,10</sup>  
A. C. S. Readhead,<sup>8</sup> J. L. Richards,<sup>11</sup> Ł. Stawarz<sup>12,13</sup> and D. Donato<sup>9,10</sup>

<sup>1</sup>Dip. di Fisica, Università degli Studi di Perugia, Via A. Pascoli, I-060123 Perugia, Italy

<sup>2</sup>INAF-Istituto di Radioastronomia, Via Gobetti 101, I-40129 Bologna, Italy

<sup>3</sup>CIFS, Viale Settimio Severo 63, I-10133 Torino, Italy

<sup>4</sup>Dip. di Astronomia, Università di Bologna, Via Ranzani 1, I-40127 Bologna, Italy

<sup>5</sup>US Naval Research Laboratory, Code 7653, 4555 Overlook Avenue SW, Washington, DC 20375-5352, USA

<sup>6</sup>INAF-Osservatorio Astronomico di Torino, Via Osservatorio 20, I-10025 Pino Torinese (TO), Italy

<sup>7</sup>Max-Planck-Institute für Radioastronomie, Auf dem Hügel 69, D-53121 Bonn, Germany

<sup>8</sup>Cahill Center for Astronomy and Astrophysics, California Institute of Technology 1200 E. California Blvd., Pasadena, CA 91125, USA

<sup>9</sup>Department of Astronomy, University of Maryland, Baltimore County, 1000 Hilltop Circle, Baltimore, MD 20742, USA

<sup>10</sup>Center for Research and Exploration in Space Science and Technology and NASA Goddard Space Flight Center, Greenbelt, MD 20771, USA

<sup>11</sup>Department of Physics, Purdue University, 525 Northwestern Avenue, West Lafayette, IN 47907, USA

<sup>12</sup>Institute of Space and Astronautical Science, JAXA, 3-1-1 Yoshinodai, Sagami-hara, Kanagawa 229-8510, Japan

<sup>13</sup>Astronomical Observatory, Jagiellonian University, ul. Orła 171, Kraków 30-244, Poland

Accepted 2012 July 11. Received 2012 June 7; in original form 2012 April 13

## ABSTRACT

We report *Fermi* Large Area Telescope (LAT) observations of the radio-loud active galactic nucleus SBS 0846+513 ( $z = 0.5835$ ), optically classified as a narrow-line Seyfert 1 galaxy, together with new and archival radio-to-X-ray data. The source was not active at  $\gamma$ -ray energies during the first two years of *Fermi* operation. A significant increase in activity was observed during 2010 October–2011 August. In particular, a strong  $\gamma$ -ray flare was observed in 2011 June reaching an isotropic  $\gamma$ -ray luminosity (0.1–300 GeV) of  $1.0 \times 10^{48}$  erg s<sup>-1</sup>, comparable to that of the brightest flat spectrum radio quasars, and showing spectral evolution in  $\gamma$  rays. An apparent superluminal velocity of  $(8.2 \pm 1.5)c$  in the jet was inferred from 2011 to 2012 Very Long Baseline Array (VLBA) images, suggesting the presence of a highly relativistic jet.

Both the power released by this object during the flaring activity and the apparent superluminal velocity are strong indications of the presence of a relativistic jet as powerful as those of blazars. In addition, variability and spectral properties in radio and  $\gamma$ -ray bands indicate blazar-like behaviour, suggesting that, except for some distinct optical characteristics, SBS 0846+513 could be considered as a young blazar at the low end of the blazar's black hole mass distribution.

**Key words:** galaxies: active – galaxies: individual: SBS 0846+513 – galaxies: nuclei – galaxies: Seyfert – gamma-rays: general.

## 1 INTRODUCTION

Active galactic nuclei (AGN) are the most luminous persistent sources of high-energy radiation in the Universe. However, only a small percentage of AGN are radio loud, and this characteristic is commonly ascribed to the presence of relativistic jets, roughly perpendicular to the accretion disc. Accretion of gas on to the super-massive black hole (SMBH) is thought to power these collimated jets, even if the nature of the coupling between the accretion disc

and the jet is still among the outstanding open questions in high-energy astrophysics (e.g. Blandford 2000; Meier 2003). Certainly relativistic jets are the most extreme example of the power that can be generated by a SMBH in the centre of an AGN, with apparent bolometric luminosities up to  $10^{49}$ – $10^{50}$  erg s<sup>-1</sup> (e.g. Ackermann et al. 2010; Bonnoli et al. 2011), and a large fraction of the power emitted in  $\gamma$  rays.

Before the launch of the *Fermi* satellite only two classes of AGN were known to generate these structures and thus to emit up to the  $\gamma$ -ray energy range: blazars and radio galaxies, both hosted in giant elliptical galaxies (Blandford & Rees 1978). The first two years of observations by the Large Area Telescope (LAT) on-board

\*E-mail: filippo.dammando@fisica.unipg.it

*Fermi* confirmed that these two are the most numerous classes of identified sources in the extragalactic  $\gamma$ -ray sky (Abdo et al. 2010a; Nolan et al. 2012), but the discovery of variable  $\gamma$ -ray emission from four radio-loud narrow-line Seyfert 1 galaxies (NLS1s) revealed the presence of a possible emerging third class of AGN with relativistic jets (Abdo et al. 2009a,b,c). In addition, *Fermi*-LAT observations gave us the opportunity to study in more detail particular subclasses of the established types of  $\gamma$ -ray-emitting AGN (e.g. broad-line radio galaxies; Abdo et al. 2010d; Kataoka et al. 2011). On the contrary, no radio-quiet Seyfert galaxies were detected in  $\gamma$  rays until now (Ackermann et al. 2012).

NLS1 are a class of AGN identified by Osterbrock & Pogge (1985) and characterized by the following optical properties: narrow permitted lines [full width at half-maximum (FWHM) ( $H\beta$ )  $< 2000 \text{ km s}^{-1}$ ] emitted from the broad-line region,  $[O \text{ III}]/H\beta < 3$  (a criterion introduced by Goodrich 1989), and a bump due to Fe II (see e.g. Pogge 2000, for a review). They also exhibit strong X-ray variability, steep X-ray spectra (photon indices  $\Gamma_X > 2$ ; Boller, Bradt & Fink 1996; Grupe et al. 2010), and substantial soft X-ray excess (Boller et al. 1996). These characteristics point to systems with smaller masses of the central BH ( $10^6$ – $10^8 M_\odot$ ; Yuan et al. 2008) than in blazars and radio galaxies and higher accretion rates (close to or above the Eddington limit; Yuan et al. 2008). NLS1 are generally radio quiet ( $R < 10$ , radio loudness  $R$  being defined as ratio of rest-frame 1.4 GHz and 4400 Å flux densities), with only a small fraction classified as radio loud ( $< 7$  per cent; Komossa et al. 2006), even more sparse ( $\sim 2.5$  per cent) are very radio-loud NLS1s ( $R > 100$ ), while generally 10–15 per cent of quasars are radio loud and very radio loud. In the past, several authors investigated the peculiarities of radio-loud NLS1s with non-simultaneous radio-to-X-ray data, suggesting similarities with the young stage of quasars or different types of blazars (Komossa et al. 2006; Yuan et al. 2008; Foschini et al. 2009). The strong and variable radio emission, and the flat radio spectrum together with variability studies suggested the presence in some radio-loud NLS1s of a relativistic jet, confirmed in some objects by the *Fermi*-LAT detection in  $\gamma$  rays (Abdo et al. 2009c). This finding poses intriguing questions about the nature of these objects, the onset of production of relativistic jets and the cosmological evolution of radio-loud AGN. The impact of peculiar characteristics of the central engines in radio-loud NLS1s, which seem quite different of those of blazars and manifest in their peculiar optical characteristics, on the  $\gamma$ -ray production mechanisms is currently under debate.

In 2011 June high  $\gamma$ -ray activity from SBS 0846+513 was observed by *Fermi*-LAT. Preliminary results were reported in Donato & Perkins (2011). That was an important confirmation of the detection of a new  $\gamma$ -ray NLS1 after the claim by Foschini (2011).<sup>1</sup>

First identified with a BL Lac object at redshift  $z = 1.86$  during a bright state by Arp et al. (1979), SBS 0846+513 is a high-redshift object positioned very close to a low-redshift galaxy at the end of a chain of five galaxies. Arp et al. (1979) noted also a small nebulosity close to SBS 0846+513 that could be a normal red galaxy observed by chance near the object due to projection effects. The Sloan Digital Sky Survey (SDSS) spectrum of the source reported in Zhou et al. (2005) is typical of NLS1:  $\text{FWHM}(H\beta) = 1710 \pm 184 \text{ km s}^{-1}$ ,  $[O \text{ III}]/H\beta \simeq 0.32$  and a strong Fe II bump. Similar values were obtained by Yuan et al. (2008) analysing the same SDSS spectrum:

$\text{FWHM}(H\beta) = 1810 \pm 191 \text{ km s}^{-1}$  and  $[O \text{ III}]/H\beta \simeq 0.31$ . Moreover, the SDSS spectrum showed that its true redshift is  $z = 0.5835$ . Nottale (1986) and others suggested that it was a gravitationally lensed quasar with variability due to gravitational amplification by a star in an intervening galaxy. However, with broader wavelength coverage and high resolution, no signs of any intervening galaxies have been found in the SDSS spectrum. The *Hubble Space Telescope* (*HST*) image, collected when SBS 0846+513 was in a faint state ( $V \sim 19.7$  mag), does not show significant resolved structure, thus no indication of the host galaxy (Maoz et al. 1993). High polarization ( $> 10$  per cent) was detected in optical and radio by Moore & Stockman (1981) and Sitko et al. (1984). A remarkable optical variability was observed in the past with an amplitude of  $\Delta V \sim 5$  mag over 1 yr and  $\Delta V \sim 4$  mag over 1 month (Arp et al. 1979). The high polarization, very high brightness temperature ( $T_b > 10^{13}$  K; Zhou et al. 2005), and the large-amplitude variability observed in optical were clues for the presence of an at least mildly relativistic jet, now confirmed by the LAT detection in  $\gamma$  rays and superluminal motion revealed by our new radio observations.

In this paper we present the detection of SBS 0846+513 in  $\gamma$  rays and discuss its characteristics by means of the available radio-to- $\gamma$ -ray data. Preliminary results about the high-resolution Very Long Baseline Array (VLBA) observations of the source were presented in Orienti, D’Ammando & Giroletti (2012). The paper is organized as follows. In Section 2 we report the LAT data analysis and results. In Section 3 we report the result of the *Swift* observations performed in 2011 August–September. Radio data collected by Medicina, Owens Valley Radio Observatory (OVRO), Effelsberg, VLBA and Very Large Array (VLA) are presented in Section 4 and discussed in Sections 5 and 6. In Section 7 we present the spectral energy distribution (SED) modelling, while discussion and concluding remarks are presented in Section 8.

Throughout the paper, a  $\Lambda$  cold dark matter ( $\Lambda$ CDM) cosmology with  $H_0 = 71 \text{ km s}^{-1} \text{ Mpc}^{-1}$ ,  $\Omega_\Lambda = 0.73$  and  $\Omega_m = 0.27$  is adopted. The corresponding luminosity distance at  $z = 0.5835$  is  $d_L = 3406 \text{ Mpc}$ , and 1 arcsec corresponds to a projected distance of 6.584 kpc.

## 2 *Fermi*-LAT DATA: SELECTION AND ANALYSIS

The *Fermi*-LAT is a  $\gamma$ -ray telescope operating from 20 MeV to  $> 300 \text{ GeV}$ . The instrument is an array of  $4 \times 4$  identical towers, each one consisting of a tracker (where the photons are pair-converted) and a calorimeter (where the energies of the pair-converted photons are measured). The entire instrument is covered with an anticoincidence detector to reject the charged-particle background. The LAT has a large peak effective area ( $\sim 8000 \text{ cm}^2$  for 1 GeV photons), an energy resolution typically  $\sim 10$  per cent, and a field of view of about 2.4 sr with an angular resolution (68 per cent containment angle) better than  $1^\circ$  for energies above 1 GeV. Further details about the LAT are given by Atwood et al. (2009).

The LAT data reported in this paper were collected over the first 40 months of *Fermi* operation, from 2008 August 4 (MJD 54682) to 2011 December 4 (MJD 55899). During this time the LAT instrument operated almost entirely in survey mode. The analysis was performed with the *SCIENCE TOOLS* software package version v9r23p1. The LAT data were extracted within a  $15^\circ$  region of interest (RoI) centred at the radio location of SBS 0846+513. Only events belonging to the ‘Source’ class were used. In addition, a cut on the zenith angle ( $< 100^\circ$ ) was also applied to reduce contamination from the Earth limb  $\gamma$  rays, which are produced by cosmic rays interacting

<sup>1</sup> The analysis presented in Foschini (2011) was performed with the P6\_V3 IRFs, starting from the first *Fermi*-LAT catalogue (1FGL) as a reference for the background sources, and over the period 2008 August–2011 February.

with the upper atmosphere. The spectral analysis (from which we derived spectral fits and photon fluxes) were performed with the post-launch instrument response functions (IRFs) P7SOURCE\_V6 using an unbinned maximum likelihood method implemented in the Science tool `GTLIKE`.

The background model used to extract the  $\gamma$ -ray signal includes a Galactic diffuse emission component and an isotropic component. The model that we adopted for the Galactic component is given by the file `gal_2year7v6_v0.fits`, and the isotropic component, which is the sum of the extragalactic diffuse emission and the residual charged-particle background, is parametrized by the file `iso_p7v6source.txt`.<sup>2</sup> The normalizations of both components in the background model were allowed to vary freely during the spectral point fitting.

We examine the significance of the  $\gamma$ -ray signal from the sources by means of the test statistics (TS) based on the likelihood ratio test. The test statistic  $TS = 2\Delta\log(\text{likelihood})$  between models with and without the source is a measure of the probability of having a  $\gamma$ -ray source at the localization specified, which compares models whose parameters have been adjusted to maximize the likelihood of the data given the model (Mattox et al. 1996). The source model used in `GTLIKE` includes all the point sources from the second *Fermi*-LAT catalogue (2FGL; Nolan et al. 2012) that fall within  $20^\circ$  from the source. The spectra of these sources were parametrized by power-law (PL) functions, except for 2FGL J0920.9+4441 and 2FGL J0957.7+5522, for which we used a log-parabola (LP) in their spectral modelling as in the 2FGL catalogue. We removed from the model the sources having  $TS < 25$  and/or fluxes below  $1.0 \times 10^{-8}$  photons  $\text{cm}^{-2} \text{s}^{-1}$  over 40 months and repeated the fit. Thus a final fitting procedure has been performed with the sources within  $10^\circ$  from SBS 0846+513 included with the normalization factors and the photon indices left as free parameters. For the sources located between  $10^\circ$  and  $15^\circ$  we kept the normalization and the photon index fixed to the values obtained in the previous fitting procedure. The RoI model includes also sources falling between  $15^\circ$  and  $20^\circ$  from the target source, which can contribute to the total counts observed in the RoI due to the energy-dependent size of the point spread function (PSF) of the instrument. For these additional sources, normalizations and indices were also fixed to the values of the 2FGL catalogue.

SBS 0846+513 was not in the 1FGL or 2FGL catalogues, indicating that the source was not detected with  $TS > 25$  in either one year or two years of *Fermi* observations (Abdo et al. 2010a; Nolan et al. 2012). Integrating over the first two years of *Fermi* operation the fit yielded a  $TS = 14$ . The  $2\sigma$  upper limit over the first 2 yr of LAT data is  $8.5 \times 10^{-9}$  photons  $\text{cm}^{-2} \text{s}^{-1}$  in the 0.1–300 GeV energy range,<sup>3</sup> assuming that the photon index is  $\Gamma = 2.3$ , which is the average value found for low-synchrotron-peaked blazars in the second LAT AGN catalogue (2LAC; Ackermann et al. 2012). On the contrary, the fit with a PL model to the data integrated over the third year of *Fermi* operation (2010 August 4–2011 August 4; MJD 55412–55777) in the 0.1–300 GeV energy range results in a  $TS = 653$ , with an integrated average flux of  $(6.7 \pm 0.5) \times 10^{-8}$  photons  $\text{cm}^{-2} \text{s}^{-1}$  and a photon index of  $\Gamma = 2.23 \pm 0.05$ .

Finally, over the period 2011 August 4–December 4 (MJD 55777–55899) only a  $TS = 8$  was obtained, with a  $2\sigma$  upper limit

of  $1.9 \times 10^{-8}$  photons  $\text{cm}^{-2} \text{s}^{-1}$  in the 0.1–300 GeV energy range, assuming that the photon index is  $\Gamma = 2.23$ . During 2011 August–December the source was not detected with  $TS > 10$  using a time bin of 1 month, indicating a significant variability in the  $\gamma$ -ray activity of the source on month time-scales. For the rest of the paper we focused on the  $\gamma$ -ray data collected over 2010 August 4–2011 August 4.

The  $\gamma$ -ray point source localization by means of the `GTFINDSRC` tool applied to the  $\gamma$  rays extracted during the third year of observation results in RA = 132°48, Dec. = +51°13 (J2000), with a 95 per cent error circle radius of 0'06, at an angular separation of 0'01 from the radio position of SBS 0846+513 (RA = 132°492, Dec. = +51°141, J2000). This implies a strict spatial association with the radio coordinates of the NLS1 SBS 0846+513. The proposed association could be questioned to some extent due to the presence of a low-redshift star-forming galaxy almost on the line of sight towards SBS 0846+513. And indeed, several members of the Local Group and also some nearby starburst galaxies have been recently detected by *Fermi*-LAT and thus established as sources of high energy photons. Their  $\gamma$ -ray luminosities range however between  $10^{40}$  and  $\sim 3 \times 10^{43}$  erg  $\text{s}^{-1}$ , and no variability in their  $\gamma$ -ray emission was observed or expected (Abdo et al. 2010e). The very large  $\gamma$ -ray luminosity of the LAT object discussed here and its flaring activity therefore rule out the foreground galaxy as the source of the detected  $\gamma$  rays.

In order to test for curvature in the  $\gamma$ -ray spectrum of SBS 0846+513 two alternative spectral models with respect to the PL were used: the LP,  $dN/dE \propto E/E_0^{-\alpha-\beta \log(E/E_0)}$  (Landau et al. 1986; Massaro et al. 2004), and the broken PL (BPL). In the case of the LP the parameter  $\alpha$  is the spectral slope at the energy  $E_0$  and the parameter  $\beta$  measures the curvature around the peak. We fixed the reference energy  $E_0$  to 300 MeV. We used a likelihood ratio test to check the PL model (null hypothesis) against the LP model (alternative hypothesis). These values may be compared, following Nolan et al. (2012), by defining the curvature test statistic  $TS_{\text{curve}} = 2(\log L_{\text{LP}} - \log L_{\text{PL}}) = 10$  corresponding to  $\sim 3.3\sigma$  difference. This value is below the threshold of  $TS_{\text{curve}} = 16$  applied in Nolan et al. (2012) for defining a significant curvature, thus suggesting only a hint of spectral curvature in the average  $\gamma$ -ray spectrum of SBS 0846+513. We tested also the BPL model, with photon indices  $\Gamma_1$  below and  $\Gamma_2$  above the break energy  $E_{\text{break}}$ . We fixed  $E_{\text{break}}$  at 1.4 GeV. This value was estimated studying the profile of the likelihood function, fixing  $E_{\text{break}}$  at different values between 100 MeV and 3 GeV with a step of 50 MeV and finding the minimum  $\log(\text{likelihood})$  value. Also for this spectral model we obtain  $TS_{\text{curve}} = 2(\log L_{\text{BPL}} - \log L_{\text{PL}}) = 10$ ; therefore, we adopt the PL for the following LAT analysis. The fit results are reported in Table 1.

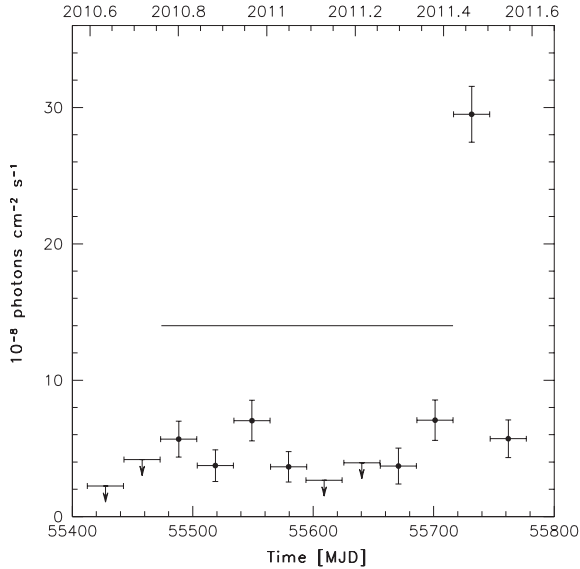
Fig. 1 shows the  $\gamma$ -ray light curve of the third year of *Fermi* observations built using 1-month time bins. For each time bin the photon index of SBS 0846+513 and all sources within  $15^\circ$  from it was frozen to the value resulting from the likelihood analysis over the entire year, while for the sources between  $15^\circ$  and  $20^\circ$  from SBS 0846+513 the photon index was frozen to the value reported in the 2FGL catalogue. If  $TS < 10$  the values of the fluxes were replaced by the  $2\sigma$  upper limits. The systematic uncertainty in the flux is energy dependent: it amounts to 10 per cent at 100 MeV, decreasing to 5 per cent at 560 MeV and increasing to 10 per cent above 10 GeV. By means of the `GTSRCPROB` tool we estimated that the highest energy photon emitted by SBS 0846+513 (with probability  $> 80$  per cent of being associated with the source) was observed on 2011 May 2 at distance of 0'34 from the source with an energy of 31 GeV.

<sup>2</sup> <http://fermi.gsfc.nasa.gov/ssc/data/access/lat/BackgroundModels.html>

<sup>3</sup> To obtain a convergence we performed the fit considering only the sources within  $10^\circ$  from SBS 0846+513 and  $E > 300$  MeV and extrapolated the flux down to 100 MeV.

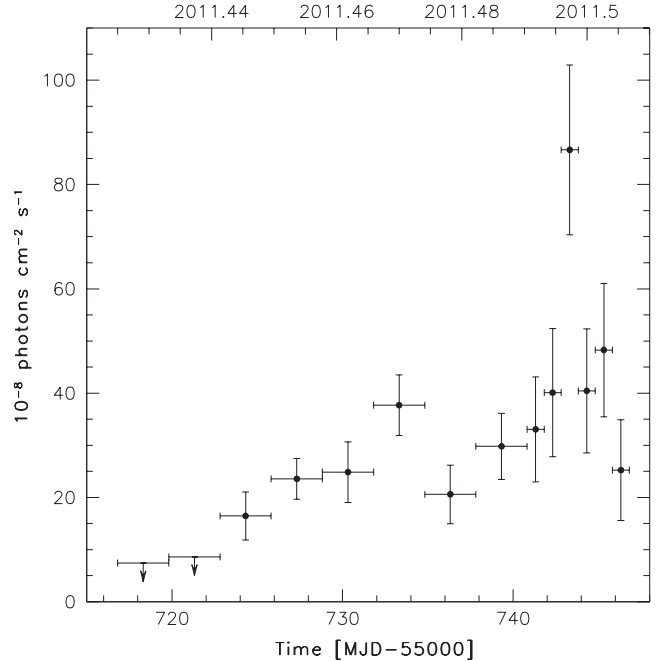
**Table 1.** Unbinned likelihood spectral fit results.

Time period (MJD)	PL	$\alpha$	LP	BPL	
	$\Gamma$		$\beta$	$\Gamma_1$	$\Gamma_2$
55 412–55777	$2.23 \pm 0.05$	$1.93 \pm 0.12$	$0.13 \pm 0.05$	$2.00 \pm 0.09$	$2.70 \pm 0.18$
55 717–55747	$1.98 \pm 0.05$	$1.23 \pm 0.19$	$0.30 \pm 0.07$	$1.51 \pm 0.12$	$2.81 \pm 0.21$

**Figure 1.** Monthly integrated flux ( $E > 100$  MeV) light curve of SBS 0846+513 obtained from 2010 August 4 to 2011 August 4. Arrows refer to  $2\sigma$  upper limits on the source flux. Upper limits are computed when  $TS < 10$ . The horizontal line indicates the period considered for the SED.

The source was not continuously detected over the entire third year and the flux remained below  $10^{-7}$  photons  $\text{cm}^{-2} \text{s}^{-1}$ , except in the period of 2011 June 4–July 4 when an increase in flux by a factor of  $\sim 4$  was observed. Considering the high activity of the source we extracted a spectrum over that period, obtaining a photon index of  $\Gamma = 1.98 \pm 0.05$  and a flux of  $(24.4 \pm 2.1) \times 10^{-8}$  photons  $\text{cm}^{-2} \text{s}^{-1}$ . A similar spectral evolution has been already observed in other flat spectrum radio quasars (FSRQs) during a bright state (Abdo et al. 2010b). A light curve focused on the period 2011 June 4–July 4, extracted with the photon index fixed to  $\Gamma = 1.98$ , was built with 3-d and 1-d time bins (Fig. 2). We used a 1-d time bin for the period with higher statistics. The peak of the emission was observed between June 30 19:43 UT and July 1 19:43 UT, with a flux of  $(87 \pm 16) \times 10^{-8}$  photons  $\text{cm}^{-2} \text{s}^{-1}$  in the 0.1–300 GeV energy range. The peak  $\gamma$ -ray flux is a factor of  $\sim 13$  higher with respect to the average flux estimated over the entire third year of observation. The  $\gamma$ -ray flare is characterized by a sharp increase in flux of a factor of  $\sim 2.5$  in 1 d and return to the previous flux level in 1 d.

For taking into consideration the possible influence of the choice of the  $T_0$  (the start time of the bin) used for building the light curve on the determination of the  $\gamma$ -ray peak, we shifted the  $T_0$  of 12 h back and forth and recalculated the daily flux, obtaining  $(53 \pm 15) \times 10^{-8}$  and  $(66 \pm 15) \times 10^{-8}$  photons  $\text{cm}^{-2} \text{s}^{-1}$ , respectively. Finally, during the month of high activity, replacing the PL with a LP or a BPL we obtain a  $TS_{\text{curve}} = 49$ , indicating a significant curvature. We noted that the curvature parameter  $\beta$  in the LP spectral model increased as the flux increased (see Table 1).

**Figure 2.** Integrated flux ( $E > 100$  MeV) light curve of SBS 0846+513 obtained from 2011 June 4 to 2011 July 4 with 3-d or 1-d time bins. Arrows refer to  $2\sigma$  upper limits on the source flux. Upper limits are computed when  $TS < 10$ .

### 3 *Swift* DATA: ANALYSIS AND RESULTS

The *Swift* satellite (Gehrels et al. 2004) performed two observations of SBS 0846+513 on 2011 August 30 and September 15 for 6.8 and 5.5 ks, respectively. The observations were performed with all three on-board instruments: the X-ray Telescope (XRT; Burrows et al. 2005, 0.2–10.0 keV), the Ultraviolet/Optical Telescope (UVOT; Roming et al. 2005, 170–600 nm) and the Burst Alert Telescope (BAT; Barthelmy et al. 2005, 15–150 keV).

The hard X-ray flux of this source is below the sensitivity of the BAT instrument for such short exposures and therefore the data from this instrument will not be used. Moreover, the source was not present in the *Swift* BAT 58-month hard X-ray catalogue (Baumgartner et al. 2010) and the 54-month Palermo BAT catalogue (Cusumano et al. 2010).

The XRT data were processed with standard procedures (`xrtpipeline v0.12.6`), filtering and screening criteria by using the `HEASOFT` package (v6.11). The data were collected in photon counting mode in both of the observations, and only XRT event grades 0–12 were selected. The source count rate was low ( $< 0.5$  counts  $\text{s}^{-1}$ ); thus pile-up correction was not required. Source events were extracted from a circular region with a radius of 20 pixel (1 pixel  $\sim 2.36$  arcsec), while background events were extracted from a circular region with radius of 50 pixel away from the source region. Ancillary response files were generated with `xrtmkarf`, and account for different extraction regions, vignetting and PSF

**Table 2.** Log and fitting results of *Swift*/XRT observations of SBS 0846+513 using a power-law model with  $N_H$  fixed to Galactic absorption.

Observation date	Net exposure time (s)	Photon index $\Gamma$	Flux 0.3–10 keV <sup>a</sup> ( $\times 10^{-13}$ erg cm <sup>-2</sup> s <sup>-1</sup> )
2011-08-03	6738	1.51 $\pm$ 0.24	9.0 $\pm$ 2.2
2011-09-15	5427	1.43 $\pm$ 0.28	7.7 $\pm$ 2.9

<sup>a</sup>Observed flux.

corrections. We used the spectral redistribution matrices v013 in the CALIBRATION data base maintained by HEASARC.

Considering the low number of photons collected (<200 counts) the spectra are rebinned with a minimum of 1 count per bin and the Cash statistics (Cash 1979) are used. We fit the spectrum with an absorbed PL using the photoelectric absorption model `tbabs` (Wilms et al. 2000), with a neutral hydrogen column fixed to its Galactic value ( $2.91 \times 10^{20}$  cm<sup>-2</sup>; Kalberla et al. 2005). The low photon statistics prevents us from fitting the X-ray data with a more complicated model than a simple PL. We noted that also in Grupe et al. (2010), in which a large sample of NLS1s observed by *Swift*/XRT was studied, the absorption column density was fixed to the Galactic value and the authors found that in the majority of NLS1s the spectrum can be fitted sufficiently well by an absorbed single PL model with negligible intrinsic absorption. The fit results are reported in Table 2. The relatively hard X-ray spectrum with respect to the other NLS1s (e.g. Grupe et al. 2010) could be due to the contribution of inverse Compton radiation from a relativistic jet, similar to FSRQs. A photon index of 1.5–1.8 was observed in X-rays also for PMN J0948+0022, the first NLS1 detected in  $\gamma$  rays by *Fermi*-LAT (Abdo et al. 2009b; Foschini et al. 2011).

In the past SBS 0846+513 was detected in X-rays only by *ROSAT*, with a 0.1–2.4 keV flux of  $2.7 \times 10^{-13}$  erg cm<sup>-2</sup> s<sup>-1</sup> and a photon index of  $\Gamma = 1.77^{+0.44}_{-0.60}$  (Yuan et al. 2008). As a comparison the flux observed on August 30 by *Swift*/XRT in the same energy range with  $\Gamma$  fixed to 1.77 is  $(3.7 \pm 0.6) \times 10^{-13}$  erg cm<sup>-2</sup> s<sup>-1</sup>,  $\sim 40$  per cent higher than the *ROSAT* observations, adding evidence of the variability character of the source.

In 2011 August the UVOT instrument took five frames in the *w1* band only, while four sequences with all *v*, *b*, *u*, *w1*, *m2* and *w2* filters were acquired in 2011 September. These data were processed with v6.10 of the HEASOFT package and the CALDB release dated 2011 August 12. Source counts were extracted from a circular region of 5 arcsec radius centred on the source, while background counts were derived from a circular region of 10 arcsec radius in the source neighbourhood. By fitting the source spectrum of September 15 with a PL, we calculated the effective wavelengths, count rate to flux conversion factors ( $CF_\Lambda$ ) and Galactic extinctions for the UVOT bands according to the procedure explained in Raiteri et al. (2010, 2011). The results are shown in Table 3. To obtain the UVOT dereddened fluxes reported in Table 4, we multiplied the count rates for the  $CF_\Lambda$  and corrected for the corresponding Galactic extinction values  $A_\Lambda$ .

We note that a *Swift*/UVOT observation performed on 2011 September 15 found SBS 0846+513 about 0.4 mag brighter in *V* band with respect to the *HST* observation in 1992 January.

## 4 RADIO DATA: ANALYSIS AND RESULTS

New and archival radio data for SBS 0846+513 were collected from Medicina, OVRO, the Effelsberg 100-m, VLA and VLBA. In

**Table 3.** Results of the UVOT calibration procedure: effective wavelengths  $\lambda_{\text{eff}}$ , count rate to flux conversion factors  $CF_\Lambda$  and Galactic extinction calculated from the Cardelli et al. (1989) laws.

Filter	$\lambda_{\text{eff}}$ (Å)	$CF_\Lambda$ ( $\times 10^{-16}$ erg cm <sup>-2</sup> s <sup>-1</sup> Å <sup>-1</sup> )	$A_\Lambda$ (mag)
<i>v</i>	5430	2.60	0.09
<i>b</i>	4360	1.47	0.11
<i>u</i>	3476	1.65	0.14
<i>uvw1</i>	2621	4.40	0.19
<i>uvm2</i>	2257	8.36	0.24
<i>uvw2</i>	2087	5.97	0.23

**Table 4.** Results of the analysis of UVOT data for SBS 0846+513.

MJD	Filter	Magnitude	Magnitude_error
55803.644	<i>uvw1</i>	19.57	0.07
55819.497	<i>v</i>	19.10	0.30
55819.489	<i>b</i>	19.67	0.19
55819.488	<i>u</i>	19.22	0.17
55819.497	<i>uvw1</i>	19.41	0.15
55819.501	<i>uvm2</i>	19.55	0.15
55819.493	<i>uvw2</i>	19.55	0.10

the following subsections we present the observations performed by these facilities.

### 4.1 Medicina

We observed SBS 0846+513 with the Medicina radio telescope five times between 2011 August and November. We used the new Enhanced Single-dish Control System (ESCS) acquisition system, which provides enhanced sensitivity and supports observations with the cross-scan technique. All observations were performed at both 5 and 8.4 GHz; the typical on-source time is 1.5 min and the flux density was calibrated with respect to 3C 286. Since the signal-to-noise ratio in each scan across the source was low (typically  $\sim 3$ ), we performed a stacking analysis of the scans, which allowed us to significantly improve the signal-to-noise ratio and the accuracy of the measurement. We list the final values of the 5 and 8.4 GHz flux density in Table 5.

### 4.2 OVRO

As part of an ongoing blazar monitoring programme, the OVRO 40-m radio telescope has observed SBS 0846+513 at 15 GHz regularly since the end of 2007 (Richards et al. 2011). This monitoring programme includes over 1500 known and likely  $\gamma$ -ray loud blazars

**Table 5.** Results of the Medicina 32-m radio observations.

Obs. date	$S_5$ (mJy)	$S_{8.4}$ (mJy)
2011-08-10	170 $\pm$ 15	235 $\pm$ 20
2011-09-08	210 $\pm$ 20	185 $\pm$ 20
2011-09-22	190 $\pm$ 20	180 $\pm$ 20
2011-10-13	190 $\pm$ 20	280 $\pm$ 30
2011-11-16	250 $\pm$ 30	275 $\pm$ 25

above declination  $-20^\circ$ . The sources in this programme are observed in total intensity twice per week with a 4 mJy (minimum) and 3 per cent (typical) uncertainty. Observations are performed with a dual-beam (each 2.5 arcmin FWHM) Dicke-switched system using cold sky in the off-source beam as the reference. Additionally, the source is switched between beams to reduce atmospheric variations. The absolute flux density scale is calibrated using observations of 3C 286, adopting the flux density (3.44 Jy) from Baars et al. (1977). This results in about a 5 per cent absolute scale uncertainty, which is not reflected in the plotted errors.

### 4.3 Effelsberg 100 m

The centimetre spectrum of SBS 0846+513 was observed with the Effelsberg 100-m telescope on 2011 April 30 (MJD 55681.8) within the framework of a *Fermi*-related monitoring programme of  $\gamma$ -ray blazars (F-GAMMA programme; Fuhrmann et al. 2007). The measurements were conducted with the secondary focus heterodyne receivers at 2.64, 8.35, 14.60 and 32.00 GHz. The observations were performed quasi-simultaneously with cross-scans, i.e. slewing over the source position, in azimuth and elevation directions, with adaptive numbers of subscans for reaching the desired sensitivity (for details, see Angelakis et al. 2008; Fuhrmann et al. 2008). Pointing offset correction, gain correction, atmospheric opacity correction and sensitivity correction have been applied to the data.

### 4.4 VLA and VLBA data

To implement the information on the flux density variability available from the single-dish observations and to study the source structure on kpc and pc scales, we analysed archival VLA and VLBA data at different frequencies obtained between 1986 and 2011. To study the proper motion we also made use of 15-GHz VLBA data from the MOJAVE programme.<sup>4</sup>

Usually SBS 0846+513 was observed with the VLA as a phase calibrator and the on-source observing time is generally quite short. Logs of VLA and VLBA observations are reported in Tables 6 and 7, respectively.

The data reduction of both VLA and VLBA data was performed following the standard procedures implemented in the National Radio Astronomy Observatory (NRAO) AIPS package. In the case of VLA data, the accuracy of the amplitude calibration was checked by means of either 3C 48 or 3C 286, and it resulted to be within 3 per cent. For the VLBA data sets, a priori amplitude calibration was derived using measurements of the system temperature and the antenna gains. Uncertainties of the amplitude calibrations were estimated to be within 5–10 per cent. For MOJAVE data we imported the fully calibrated  $uv$  data sets (Lister et al. 2009).

The final VLA and VLBA images were produced after a number of phase-only self-calibration iterations. The source parameters, such as flux density and angular size, were derived on the radio image plane by means of the AIPS task JMFIT which performs a Gaussian fit to the source and its subcomponents (Table 8). For the extended component visible at 15 GHz, we determine the flux density by means of TVSTAT, which performs an aperture integration on a selected region on the image plane.

<sup>4</sup> The MOJAVE data archive is maintained at <http://www.physics.purdue.edu/MOJAVE>.

**Table 6.** Log of the archival VLA observations and flux density.

Freq. (GHz)	Date	Code	Obs. time (min)	Beam (arcsec $\times$ arcsec)	Flux (mJy)
1.4	1986-04-10	AV127	9.16	$1.40 \times 1.12$	$194 \pm 6$
4.8	1986-04-10	AV127	9.16	$0.44 \times 0.35$	$286 \pm 9$
4.8	1996-01-05	BW021	1.66	$1.39 \times 1.19$	$332 \pm 10$
4.8	1996-12-30	BA018	3.33	$0.43 \times 0.36$	$363 \pm 11$
4.8	2009-05-09	CALSUR	0.66	$2.12 \times 1.18$	$196 \pm 6$
8.4	1995-08-13	AM484	0.5	$0.24 \times 0.22$	$356 \pm 11$
8.4	1995-09-02	AM484	0.5	$0.32 \times 0.23$	$327 \pm 10$

**Table 7.** Log of the VLBA observations analysed in this paper and total flux density.

Freq. (GHz)	Date	Code	Beam (mas $\times$ mas)	Obs. time (min)	Flux (mJy)
5.0	1995-03-15	BW015	$3.99 \times 1.34$	50	$284 \pm 20$
5.0	1996-01-06	BW021	$4.13 \times 1.29$	50	$281 \pm 20$
8.4	2011-03-12	BC196J	$2.00 \times 0.97$	10	$210 \pm 16$
15.3	2011-05-26	BL149DI <sup>a</sup>	$0.77 \times 0.59$	30	$244 \pm 17$
15.3	2011-07-15	BL149DM <sup>a</sup>	$0.76 \times 0.60$	30	$213 \pm 15$
15.3	2012-01-02	BL178AE <sup>a</sup>	$0.74 \times 0.64$	36	$231 \pm 21$

<sup>a</sup>Data from the MOJAVE programme.

**Table 8.** Flux density in mJy of the components of SBS 0846+513 from VLBA data. Epochs of the observations are reported in Table 7.

	E	W	W1	W2
S <sub>5</sub> GHz, ep1	$14 \pm 2$	$269 \pm 19$	–	–
S <sub>5</sub> GHz, ep2	$17 \pm 2$	$265 \pm 18$	–	–
S <sub>8.4</sub> GHz	$14 \pm 2$	$196 \pm 14$	–	–
S <sub>15.3</sub> GHz, ep1	$3.4 \pm 0.4$	$192 \pm 15$	$140 \pm 10$	$52 \pm 4$
S <sub>15.3</sub> GHz, ep2	$3.1 \pm 0.3$	$240 \pm 24$	$175 \pm 17$	$65 \pm 6$
S <sub>15.3</sub> GHz, ep3	$3.6 \pm 0.4$	$209 \pm 20$	$151 \pm 15$	$58 \pm 5$

## 5 RADIO VARIABILITY

Multi-epoch studies of the radio emission of SBS 0846+513 show significant flux density variability. In Fig. 3 we report the OVRO observations obtained since the launch of *Fermi*. From the analysis of the OVRO light curve at 15 GHz it is clear that high and low activity states are interspersed. Interestingly, no  $\gamma$ -ray emission was detected during the major radio flaring episodes that occurred before 2011. A maximum flux density variation of a factor of  $\sim 2.0$  was observed over 3 months during the period of 2010 August–2011 August, while in the period of 2008 August–2010 August a variation of a factor of  $\sim 2.8$  was observed over a similar time interval.

Flux density variability is detected also at 4.8 GHz, where the flux density varies about 70 per cent during the time interval spanned by the VLA data (1986–2009). However, the poor time coverage of the VLA data does not allow us to fully characterize the flux density behaviour on such a long time interval.

The detection of the  $\gamma$ -ray flare in 2011 June triggered a monitoring campaign with the Medicina telescope. In Fig. 4 we report the Medicina flux density at 5 (triangles) and 8.4 GHz (squares) in addition to the OVRO 15-GHz data (open circles) collected between 2011 July 28 and November 19. From August 20 (MJD 55793.628), i.e. about one month after the  $\gamma$ -ray flare, the flux density at 15 GHz started to increase reaching the maximum of about 280 mJy around

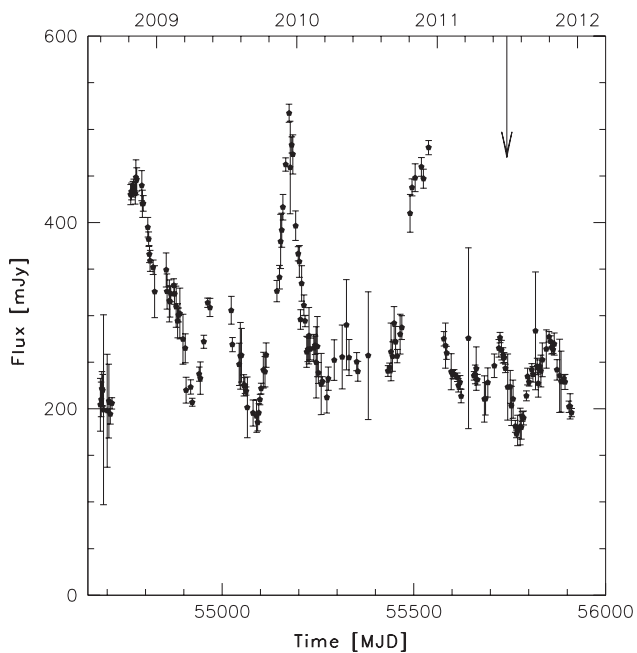


**Figure 3.** 15 GHz radio light curve for the period 2008 August 4–2011 December 12 from the OVRO telescope. The downward arrow indicates the time of the peak of the  $\gamma$ -ray activity observed by *Fermi*-LAT.

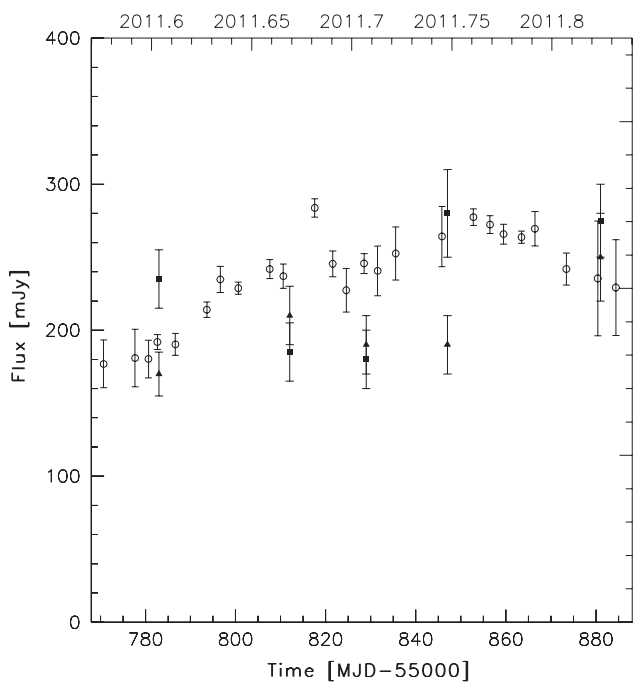


**Figure 4.** Radio data of SBS 0846+513 collected at 5.0 GHz (triangles) and 8.4 GHz (squares) by Medicina, and 15 GHz (open circles) by OVRO during the period 2011 July 28–November 19 (MJD 55770–55884).

October 18, and then it started to decrease. At lower frequencies the flux density variation is observed after a longer time, first at 8.4 GHz (October 13), and then at 5 GHz (November 16). This time delay may be explained by opacity effects, which are more severe at longer wavelengths. During this time interval also the shape of the radio spectrum changes, as is clearly visible in Fig. 5 (left-hand panel). We must note that Medicina and OVRO observations are not strictly simultaneous and to build the radio spectrum we considered

the OVRO observation that is the closest in time to the Medicina observing epoch. For comparison, in Fig. 5 (right-hand panel) we show the simultaneous radio spectrum between 2.64 and 32 GHz obtained by Effelsberg on 2011 April 30, i.e. before the high activity state detected in  $\gamma$  rays.

## 6 RADIO MORPHOLOGY

The resolution of the VLA is not adequate to resolve the radio structure of SBS 0846+513 (Fig. 6) even when the array is in its most extended configuration ( $\text{FWHM} \leq 0.3$  arcsec). When imaged with the high spatial resolution of the VLBA the source is resolved in two components with a core–jet structure (Figs 7 and 8), as also pointed out in a previous work by Taylor et al. (2005). The core (component W) is still unresolved with an upper limit of 0.3 mas, while the jet structure (component E) is  $3.5 \times 1.6$  mas. The flux density ratio between components E and W is  $\sim 19$  and 14 at 5 and 8.4 GHz, respectively. Their separation is about 3.5 mas, corresponding to  $\sim 23$  pc projected distance, given the source’s redshift. At 15 GHz component E shows an extended low-surface brightness structure with a steep spectrum. On the other hand, component W is resolved into two compact components (labelled W1 and W2 in Fig. 9). To investigate a possible proper motion of the jet, we compared the separation between W1, considered the core region, and W2, assumed to be a knot in the jet, at the three observing epochs. To this purpose, in addition to the data analysis on the image plane, we model-fitted the visibility data using Gaussian components of the three-epoch MOJAVE data by means of the model-fitting option in *DIFMAP*. This approach is preferable in case we want to derive small variations in the source structure and little changes in the position of the source components. From this comparison we found that W1 and W2 are separating with an apparent velocity of  $(0.38 \pm 0.07)$  mas yr $^{-1}$  (Fig. 10), which corresponds to  $(8.2 \pm 1.5)c$ . This apparent superluminal velocity suggests the presence of boosting effect. However, the availability of only three observing epochs spanning a short time baseline without frequent time sampling implies large uncertainties on the estimated values.

When we compare the total flux density derived from VLBA data with that from the VLA, we find that the VLBA can recover at most 85 per cent of the VLA flux density, even when the observations were performed simultaneously (i.e. 1996 January 6). This may be related to the slightly different observing frequencies, i.e. 4.8 GHz at the VLA, whereas it is 5.0 GHz at the VLBA. However, in this case the spectral index would have to be extremely steep ( $\alpha_r \sim 4$ ;  $f_v \propto \nu^{-\alpha_r}$ ) to obtain such a difference in the flux density, making this explanation unlikely. Another possibility is related to observational limitations due to the lack of short spacings of the VLBA array, implying that only structures smaller than  $\sim 40$  and 30 mas at 5 and 8.4 GHz can be detected. This suggests that the missing flux on the pc scale may be related to extended, low-surface brightness features like a jet component resolved out by the VLBA array.

## 7 SED MODELLING

The  $\gamma$ -ray detection of the radio-loud NLS1s has given us the possibility of studying the characteristics of this class of objects by modelling their broad-band spectra.

We have built a non-simultaneous SED, all of which is based on non-flaring data. This ought to adequately represent the emission from this object in a low state. The LAT spectrum was built with data centred on 2010 October 4–2011 June 4 (MJD 55473–55716). In addition we included in the SED the Effelsberg radio data collected on 2011 April 30 and the *Swift* (UVOT and XRT) data

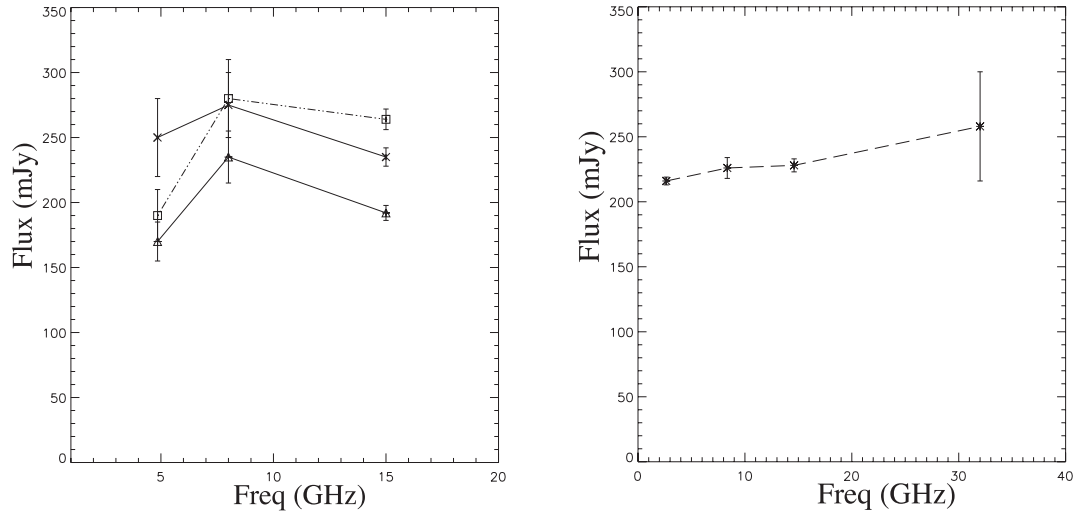


**Figure 5.** Left-hand panel: radio spectra of SBS 0846+513. Observations at 5 and 8.4 GHz are from the Medicina single-dish telescope, those at 15 GHz are from OVRO. Triangles, squares and crosses refer to observations performed around 2011 August 10, October 13 and November 16, respectively. Right-hand panel: radio spectrum of SBS 0846+513 obtained by the Effelsberg single dish on 2011 April 30 from 2.64 to 32 GHz.

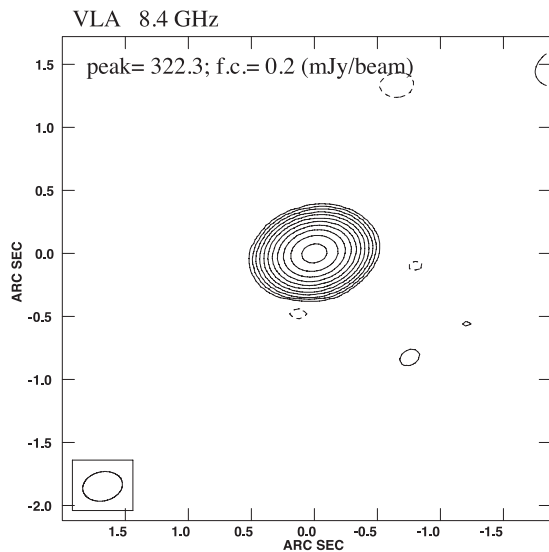


**Figure 6.** VLA image at 8.4 GHz of SBS 0846+513. On the image we provide the peak flux density, in mJy beam<sup>-1</sup>, and the first contour intensity (f.c., in mJy beam<sup>-1</sup>) that corresponds to three times the noise measured on the image plane. Contour levels increase by a factor of 2. The beam is plotted on the bottom left-hand corner of the image.

collected on 2011 September 15, thus well before and after the  $\gamma$ -ray flare. The data from Two Micron All Sky Survey (2MASS) Point Source Catalog and *WISE* preliminary release Source Catalogue provided information about the infrared (IR) part of the spectrum. The flare centred on  $\sim$ MJD 55750 had a variability time-scale of  $\sim$ 1 d, which constrains the size of the emitting region during the flare.

We modelled the SED assuming emission from a relativistic jet with mechanisms of synchrotron, synchrotron self-Compton (SSC) and Compton scattering of a dust torus external to the jet. The description of the model can be found in Finke, Dermer & Böttcher (2008) and Dermer et al. (2009). Jet powers were calculated assuming a two-sided jet. Although the flaring time-scale does not constrain the emitting region during the low state, we have produced a model fit which is roughly consistent with

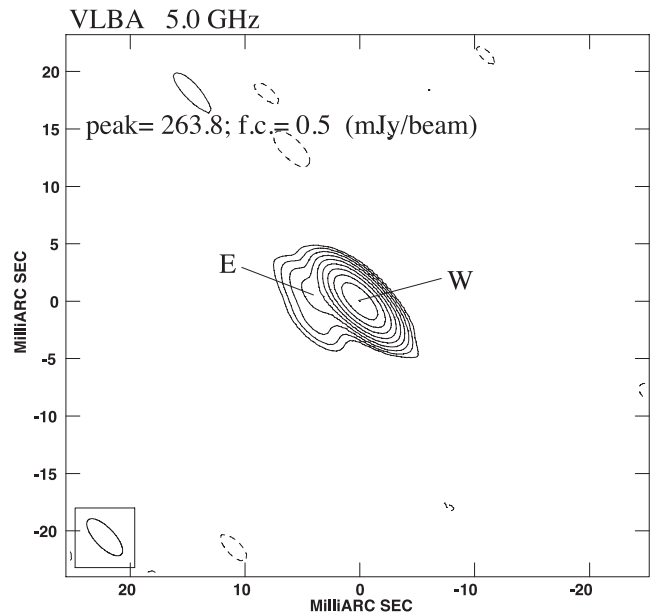


**Figure 7.** VLBA image at 5.0 GHz of SBS 0846+513. On the image we provide the peak flux density, in mJy beam<sup>-1</sup>, and the first contour intensity (f.c., in mJy beam<sup>-1</sup>) that corresponds to three times the noise measured on the image plane. Contour levels increase by a factor of 2. The beam is plotted on the bottom left-hand corner of the image.

this time-scale (about 1 d). The synchrotron component can adequately explain the IR through UV points, although some of the 2MASS points are significantly higher than the rest, and are not well fitted. This is probably due to contamination by IR emission from the host galaxy. We note that this IR excess could be consistent with the typical starlight expected from an elliptical galaxy. The radio spectrum is flat in  $F_\nu$  (Fig. 5) and probably the result of a superposition of several jet components (e.g. Konigl 1981), so for our purposes these points are considered upper limits. The synchrotron component we use is self-absorbed below  $\sim 10^{12}$  Hz. An attempt was made to fit the X-ray through  $\gamma$ -ray data with an SSC component, but this was not found to be possible. Instead, an external component was required. Correlations

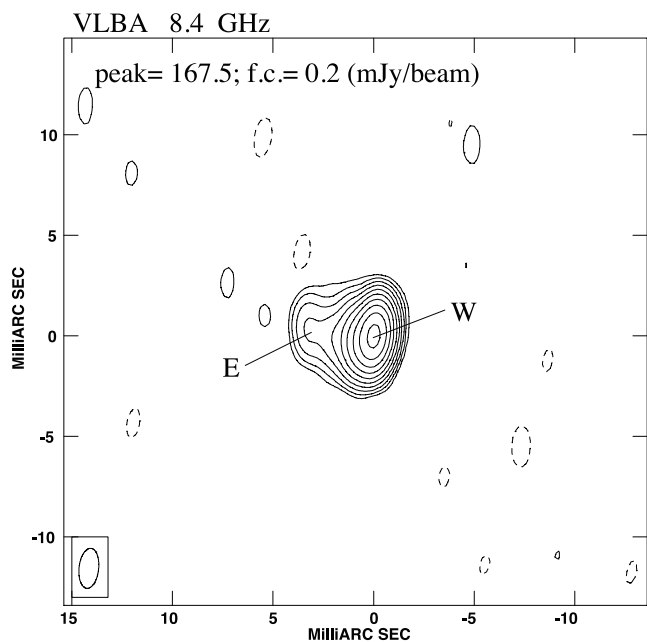


**Figure 8.** VLBA image at 8.4 GHz of SBS 0846+513. On the image we provide the peak flux density, in  $\text{mJy beam}^{-1}$ , and the first contour intensity (f.c., in  $\text{mJy beam}^{-1}$ ) that corresponds to three times the noise measured on the image plane. Contour levels increase by a factor of 2. The beam is plotted on the bottom left-hand corner of the image.

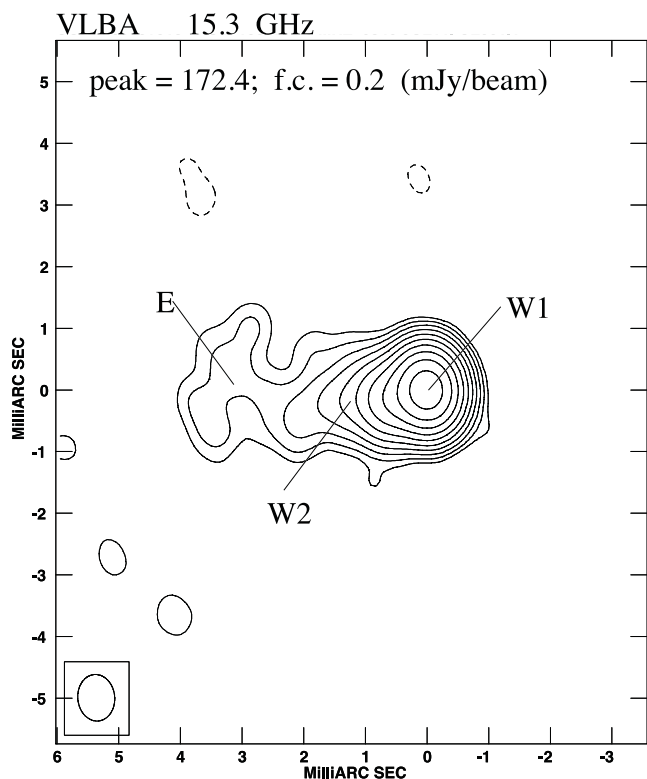


**Figure 9.** VLBA image at 15.3 GHz of SBS 0846+513. Data are from the MOJAVE programme. On the image we provide the peak flux density, in  $\text{mJy beam}^{-1}$ , and the first contour intensity (f.c., in  $\text{mJy beam}^{-1}$ ) that corresponds to three times the noise measured on the image plane. Contour levels increase by a factor of 2. The beam is plotted on the bottom corner of the image.

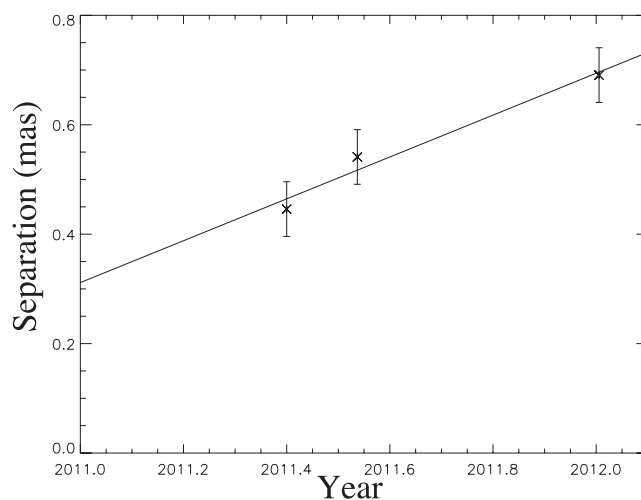


**Figure 10.** Changes in separation with time between components W1 and W2. The solid line represents the regression fit to the 15-GHz MOJAVE data.

of  $\gamma$ -ray and optical flares with radio light curves and rotations of optical polarization angles in low-synchrotron-peaked blazars seem to indicate that the  $\gamma$ -ray/optical-emitting region is outside the broad-line region, where the dust torus is the likely seed photon source (e.g. Marscher et al. 2010). So we chose as our seed photon source a dust torus, which was simulated as a one-dimensional ring with radius  $R_{\text{dust}}$  aligned orthogonal to the jet, emitting as a blackbody with temperature  $T_{\text{dust}}$  and luminosity  $L_{\text{dust}}$ . Observational evidence for a dust torus in NLS1s as well as in the other Seyfert galaxies was recently reported in Mor & Netzer (2012). The fit can be seen in Fig. 11 and the parameters can be found in Table 9. A description of the parameters can be found in Dermer et al. (2009). The dust parameters were chosen so that  $R_{\text{dust}}$  is roughly consistent with the sublimation radius (Nenkova et al. 2008), assuming that the torus luminosity is about 1/10 of the disc luminosity. If the emitting region takes up the entire width of the jet, and the jet is assumed

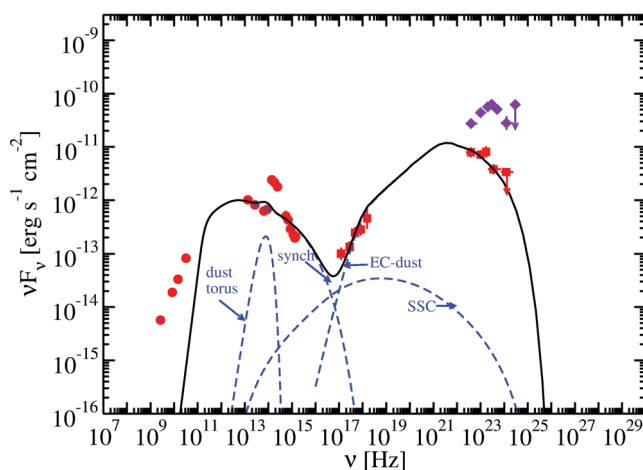


**Figure 11.** Spectral energy distribution data (circles and squares) and model fit (solid curve) of SBS 0846+513 with the model components shown as dashed curves. The data points were collected by Effelsberg (2011 April 30), *Swift* (UVOT and XRT; 2011 September 15) and *Fermi*-LAT (2010 October 4–2011 June 4), together with archival data from 2MASS and WISE. The LAT spectrum during the flaring period (2011 June 4–July 4) is shown as the diamonds.

**Table 9.** Model parameters for the SED shown in Fig. 11.

Redshift	$z$	0.5835
Bulk Lorentz factor	$\Gamma$	15
Doppler factor	$\delta_D$	15
Magnetic field	$B$	1.0 G
Variability time-scale	$t_v$	$1 \times 10^5$ s
Comoving radius of blob	$R'_b$	$2.8 \times 10^{16}$ cm
Jet height	$r$	$1.6 \times 10^{18}$ cm
Low-energy electron spectral index	$p_1$	2.2
High-energy electron spectral index	$p_2$	3.2
Minimum electron Lorentz factor	$\gamma'_{\min}$	5.0
Break electron Lorentz factor	$\gamma'_{\text{brk}}$	$3.0 \times 10^2$
Maximum electron Lorentz factor	$\gamma'_{\max}$	$9.0 \times 10^3$
Dust torus luminosity	$L_{\text{dust}}$	$4.0 \times 10^{44}$ erg s $^{-1}$
Dust torus temperature	$T_{\text{dust}}$	$1.5 \times 10^3$ K
Dust torus radius	$R_{\text{dust}}$	$2.0 \times 10^{18}$ cm
Jet power in magnetic field	$P_{j,B}$	$1.4 \times 10^{45}$ erg s $^{-1}$
Jet power in electrons	$P_{j,\text{par}}$	$4.3 \times 10^{44}$ erg s $^{-1}$

to be conical, its half-opening angle would be about  $1^\circ$ , approximately consistent with those measured from VLBI observations of blazars (Jorstad et al. 2005). This size scale is roughly the same as for the 15 GHz core (Fig. 9), and so if this model fit is correct, the  $\gamma$ -ray-emitting region is probably located near this region, which is presumably a synchrotron self-absorption photosphere.

The electron distribution used, a BPL with index  $p_1 = 2.2$  below the break at  $\gamma'_{\text{brk}}$  and  $p_2 = 3.2$  for  $\gamma'_{\text{brk}} < \gamma'$ , is consistent with particles injected with index 2.2, and emission taking place in the *slow-cooling regime* (e.g. Böttcher & Dermer 2002). That is, particles are injected between  $\gamma'_{\min}$  and  $\gamma'_{\max}$ , with a cooling break at

$$\gamma'_{\text{brk}} \equiv \frac{3m_e c^2}{4c\sigma_T t_{\text{esc}} u_{\text{tot}}},$$

where  $u_{\text{tot}}$  is the total energy density in the blob frame, which in the case of our model fit is dominated by the external energy density. The escape time  $t_{\text{esc}} \approx R'_b/c$  so that for our model fit  $\gamma'_{\text{brk}} \sim 300$ . Also note that in this model fit the magnetic field and electrons are nearly in equipartition.

Using the SDSS Data Release (DR) 1, Zhou et al. (2005) estimated the BH mass from several methods, the  $H\beta$  broad line, the  $[O_{\text{III}}]\lambda 5007$  narrow line and the host galaxy’s bulge luminosity, as  $\simeq 8.2 \times 10^6$ ,  $\simeq 5.2 \times 10^7$  and  $\simeq 4.3 \times 10^7 M_\odot$ , respectively. Large uncertainties (0.4–0.7 dex) are associated with these techniques (Verstergaard 2004). Shen et al. (2011) estimated the BH mass based on the  $H\beta$  broad line and Mg II line in the SDSS DR7 spectrum as  $\log(M_{\text{BH}}/M_\odot) = 7.99 \pm 0.12$  and  $\log(M_{\text{BH}}/M_\odot) = 7.79 \pm 0.16$ , respectively. Note that the broad-band SED shows no evidence for a blue bump, so the optical spectrum probably has considerable contamination from jet emission not taken into account in Shen et al. (2011), and so these mass estimates should be taken with caution. If the Zhou et al. (2005)  $H\beta$  estimate is correct, the total jet power will exceed the Eddington luminosity for this source [ $L_{\text{Edd}} = 1.3 \times 10^{45}$  erg s $^{-1}$   $M_{\text{BH}}/(10^7 M_\odot)$ ]. Thus the BH mass is probably more on the high side of these estimates, if the jet power is Eddington limited.

The Compton dominance for SBS 0846+513, i.e. the ratio of the peak luminosities of the Compton and synchrotron components, is  $\approx 7$ , which is a rather standard value for FSRQs, although quite a high value for BL Lacs (e.g. Finke 2012; Giommi et al. 2012). Its SED in many ways resembles that of a FSRQ, with an X-ray spectral index  $\sim 1.5$ , consistent with values for FSRQs in the BAT (Ajello

et al. 2009) and *BeppoSAX* (Donato, Sambruna & Gliozzi 2005) catalogues. As we discuss in Section 8, its LAT flux and spectral index are also consistent with values for FSRQs.

The flaring LAT spectrum is also shown in Fig. 11. Unfortunately, there are no multiwavelength data simultaneous to this flare. For FSRQs,  $\gamma$ -ray flares are often associated with optical flares, although there are occasions when they are not. Both types of flares are seen, for example, from the FSRQ PKS 1510–089 (Marscher et al. 2010) so we can only guess at the behaviour of SBS 0846+513 during this flare. However, note that during the flare, the object reaches a luminosity of  $L_{\gamma,\text{iso}} \sim 1.0 \times 10^{48}$  erg s $^{-1}$ , making the radiative power  $L_{\gamma,\text{rad}} \sim L_{\gamma,\text{iso}}/\Gamma^2 \sim 4.4 \times 10^{45}$  erg s $^{-1}$ , assuming  $\Gamma = 15$ . This is about 1/2 of the Eddington luminosity for a  $10^7 M_\odot$  BH.

## 8 DISCUSSION AND CONCLUDING REMARKS

After the four objects detected by *Fermi*-LAT in the first year of operation (Abdo et al. 2009c), SBS 0846+513 is a new NLS1 detected by *Fermi*-LAT during high  $\gamma$ -ray activity in 2011 June (Donato & Perkins 2011). The power released by this object during the flaring activity was a strong indication of the presence of a relativistic jet as powerful as those in blazars, supported by the apparent superluminal velocity of the jet derived by tracking the position of a jet component in 2011–2012 VLBA data (see Section 6). Before the  $\gamma$ -ray flaring episode, the simultaneous multifrequency observations performed by Effelsberg showed a flat radio spectrum up to 32 GHz. After the flare, the spectral shape changed, becoming convex. The spectral variability was also accompanied by variations in the radio flux density, which were originally detected at the higher frequencies, later moving to lower frequencies, likely due to opacity effects. These spectral and variability properties indicate blazar-like behaviour, which has already been observed in other  $\gamma$ -ray NLS1s (Fuhrmann et al. 2011).

Ghisellini et al. (2008, 2011), investigating the  $\gamma$ -ray properties of blazars detected by *Fermi*-LAT in the first year of observation, suggested a transition between BL Lac objects and FSRQs that can be justified mainly by the different accretion regimes: highly sub-Eddington in the former case, near-Eddington in the latter. In this context the high accretion rate of SBS 0846+513, and more generally of the  $\gamma$ -ray radio-loud NLS1s, is another indication of its similarity with FSRQs. A comparison of the BL Lacs and FSRQs from the First LAT AGN Catalogue (1LAC; Abdo et al. 2010c) with ‘misaligned AGN’ detected by *Fermi* (MAGN; non-blazar AGN with jets pointed away from the observer) in the  $\Gamma_\gamma$ - $L_\gamma$  plane has shown that MAGN and blazars occupy different regions of the plane, with only two high-redshift FR II galaxies, 3C 207 and 3C 380, which lie among the FSRQs (Abdo et al. 2010d). This is in agreement with the idea that MAGN are less beamed than blazars. In this context it is interesting to consider also the  $\gamma$ -ray NLS1s. For a direct comparison with the results shown in Abdo et al. (2010d) we calculated the flux and photon index over the third year of *Fermi* operation in the 0.1–10 GeV energy band, resulting in  $\Gamma_\gamma = 2.19 \pm 0.06$  and flux (0.1–10 GeV) =  $(6.6 \pm 0.6) \times 10^{-8}$  erg cm $^{-2}$  s $^{-1}$ . The corresponding observed isotropic  $\gamma$ -ray luminosity in the 0.1–10 GeV is  $3.6 \times 10^{46}$  erg s $^{-1}$ . We plotted these values of SBS 0846+513 in the  $\Gamma_\gamma$ - $L_\gamma$  plane together with the FSRQs, BL Lacs and misaligned AGN from Abdo et al. (2010d). As can be seen SBS 0846+513 lies in the blazar region, in particular in the transition region between the distribution of BL Lacs and FSRQs (Fig. 12). We note that also the other  $\gamma$ -ray NLS1 observed in flaring activity, PMN J0948+0022 ( $\Gamma_\gamma = 2.26 \pm 0.08$  and 0.1–10 GeV luminosity of  $9.6 \times 10^{46}$  erg s $^{-1}$  over the first 24-month of *Fermi* operation; Grandi 2011), occupies

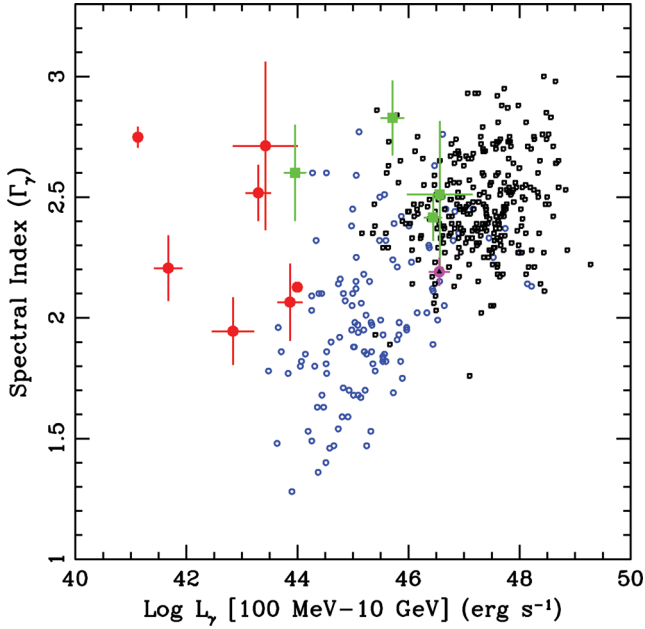


**Figure 12.** The photon index  $\Gamma_\gamma$  of FRI radio galaxies (red circles), FR II radio galaxies (green squares), BL Lacs (open blue circles) and FSRQs (open black squares) are plotted together with the NLS1 SBS 0846+513 (magenta point including a black triangle) as a function of the observed isotropic  $\gamma$ -ray luminosity (100 MeV–10 GeV). Adapted from Abdo et al. (2010d).

the same blazar region in that plane. This should reflect a similar viewing angle with respect to the jet axis and beaming factors for the  $\gamma$ -ray emission between blazars and the two  $\gamma$ -ray NLS1s SBS 0846+513 and PMN J0948+0022. In the same way the spectral evolution during the flaring activity in June 2011 observed in  $\gamma$  rays from SBS 0846+513 is a common behaviour in bright FSRQs and low-synchrotron-peaked BL Lacs detected by *Fermi* (Abdo et al. 2010b), with a change in photon index  $<0.2$ – $0.3$  and an increasing spectral curvature.

One of the key questions is the maximum power released by the jets of NLS1s. During the  $\gamma$ -ray flaring activity observed in 2011 June–July SBS 0846+513 reached an observed isotropic  $\gamma$ -ray luminosity (0.1–300 GeV) of  $1.0 \times 10^{48}$  erg s $^{-1}$  on daily time-scales, comparable to that of luminous FSRQs. After PMN J0948+0022 (Foschini et al. 2011), this is the second NLS1 observed to generate such a high power. This could be an indication that all the radio-loud NLS1s are able to host relativistic jets as powerful as those in blazars, despite the lower BH mass; alternatively some NLS1s could have peculiar characteristics allowing the development of these relativistic jets. The mechanism at work for producing a relativistic jet is not clear, and the physical parameters that drive jet formation are still under debate. One fundamental parameter could be the BH mass, with only large masses allowing for the efficient formation of a relativistic jet. It was, for example, noted by some authors (McLure & Jarvis 2004; Liu et al. 2006; Sikora, Stawarz & Lasota 2007) that quasars with  $M_{\text{BH}} > 10^8 M_\odot$  reach radio loudness three orders of magnitude greater than quasars with  $M_{\text{BH}} < 3 \times 10^7 M_\odot$ . The large radio loudness of SBS 0846+513 could challenge this idea if the BH masses estimated by Zhou et al. (2005) are confirmed. According to the ‘modified spin paradigm’ discussed in Sikora et al. (2007), another fundamental parameter for the efficiency of a relativistic jet production should be the BH spin, with

SMBHs in elliptical galaxies having on average much larger spins than SMBHs in spiral galaxies. This is due to the fact that spiral galaxies are characterized by multiple accretion events with random orientation of angular momentum vectors and small increments of mass, while elliptical galaxies underwent at least one major merger with large matter accretion triggering an efficient spin-up of the SMBH. The accretion rate (thus the mass) and the spin of the BH may be related to the host galaxy, leading to the hypothesis that relativistic jets can develop only in elliptical galaxy (e.g. Marscher 2009).

In this context the discovery of relativistic jets in a class of AGN usually hosted by spiral galaxies, such as the NLS1s, was a great surprise. Unfortunately only very sparse observations of the host galaxy of radio-loud NLS1s are available at this time, and the sample of objects studied by Deo et al. (2006) and Zhou et al. (2006) had  $z < 0.03$  and  $z < 0.1$ , respectively, including both radio-quiet and radio-loud objects. We note that BH masses of radio-loud NLS1s are generally larger with respect to the entire sample of NLS1s [ $M_{\text{BH}} \approx (2\text{--}10) \times 10^7 M_\odot$ ; Komossa et al. 2006], even if still small when compared to radio-loud quasars. The larger BH masses of radio-loud NLS1s with respect to radio-quiet NLS1s could be related to prolonged accretion episodes that can spin up the BHs. The small fraction of radio-loud NLS1s with respect to radio-loud quasars could be an indication that in the former the high accretion usually does not last sufficiently long to significantly spin up the BH (Sikora 2009).

Of the  $\gamma$ -ray-emitting NLS1s, host galaxy imaging is available only for 1H 0323+342, with *HST* and the Nordic Optical Telescope. These observations reveal a one-armed galaxy morphology or a circumnuclear ring, suggesting two possibilities: the spiral arms of the host galaxy (Zhou et al. 2007) or the residual of a merging galaxy (Anton, Browne & Marcha 2008). No significant resolved structures have been observed by *HST* for SBS 0846+513 (Maoz et al. 1993), and no high-resolution observations are available for the remaining  $\gamma$ -ray NLS1s. Thus the possibility that the development of relativistic jets in these objects could be due to strong merger activity is not ruled out. Further high-resolution observations of the host galaxies of  $\gamma$ -ray NLS1s will be fundamental to obtain important insights into relativistic jet formation and development.

To conclude, SBS 0846+513 shows all the characteristics of the blazar phenomenon. The extreme power released by SBS 0846+513 during the high  $\gamma$ -ray activity in 2011 July confirms that, as with PMN J0948+0022, NLS1s can host relativistic jets as powerful as blazars. Radio and  $\gamma$ -ray data collected for SBS 0846+513 suggest spectral and variability properties similar to blazars, and the modelling of the average SED gives similar results to those of blazars, including similar Lorentz factors. This could be an indication that these  $\gamma$ -ray NLS1s are low-mass (and possibly younger) version of blazars. The detection of new radio-loud NLS1s in  $\gamma$  rays by *Fermi*-LAT will be important for extending the source sample, and better characterizing this new class of  $\gamma$ -ray-emitting AGN. Equally important will be to perform further multifrequency observations of the  $\gamma$ -ray-emitting NLS1s already detected by *Fermi* and investigate in detail their characteristics over the entire electromagnetic spectrum, to help understand their nature.

## ACKNOWLEDGMENTS

The *Fermi* LAT Collaboration acknowledges generous ongoing support from a number of agencies and institutes that have

supported both the development and the operation of the LAT as well as scientific data analysis. These include the National Aeronautics and Space Administration and the Department of Energy in the United States, the Commissariat à l'Énergie Atomique and the Centre National de la Recherche Scientifique/Institut National de Physique Nucléaire et de Physique des Particules in France, the Agenzia Spaziale Italiana and the Istituto Nazionale di Fisica Nucleare in Italy, the Ministry of Education, Culture, Sports, Science and Technology (MEXT), High Energy Accelerator Research Organization (KEK) and Japan Aerospace Exploration Agency (JAXA) in Japan, and the K. A. Wallenberg Foundation, the Swedish Research Council and the Swedish National Space Board in Sweden. Additional support for science analysis during the operations phase is gratefully acknowledged from the Istituto Nazionale di Astrofisica in Italy and the Centre National d'Études Spatiales in France.

We thank the *Swift* team for making these observations possible, the duty scientists and science planners. This research has made use of data from the MOJAVE data base that is maintained by the MOJAVE team (Lister et al. 2009). The OVRO 40-m monitoring program is supported in part by NASA grants NNX08AW31G and NNX11A043G, and NSF grants AST-0808050 and AST-1109911. This paper is partly based on observations with the 100-m telescope of the MPIfR (Max-Planck-Institut für Radioastronomie) at Effelsberg and the Medicina telescope operated by INAF–Istituto di Radioastronomia. We acknowledge A. Orlati, S. Righini and the Enhanced Single-dish Control System (ESCS) Development Team. We acknowledge financial contribution from agreement ASI-INAf I/009/10/0. This publication makes use of data products from the Two Micron All Sky Survey, which is a joint project of the University of Massachusetts and the Infrared Processing and Analysis Center/California Institute of Technology, funded by the National Aeronautics and Space Administration and the National Science Foundation. This publication makes use of data products from the Wide-field Infrared Survey Explorer, which is a joint project of the University of California, Los Angeles, and the Jet Propulsion Laboratory/California Institute of Technology, funded by the National Aeronautics and Space Administration. We thank the anonymous referee for useful suggestions. FD would like to thank Gino Tosti and Marco Ajello for fruitful comments and discussions, and Paola Grandi who has made the data of her paper available.

## REFERENCES

- Abdo A. A. et al., 2009a, *ApJ*, 699, 976  
 Abdo A. A. et al., 2009b, *ApJ*, 707, L142  
 Abdo A. A. et al., 2009c, *ApJ*, 707, 727  
 Abdo A. A. et al., 2010a, *ApJS*, 188, 405  
 Abdo A. A. et al., 2010b, *ApJ*, 710, 1271  
 Abdo A. A. et al., 2010c, *ApJ*, 715, 429  
 Abdo A. A. et al., 2010d, *ApJ*, 720, 912  
 Abdo A. A. et al., 2010e, *A&A*, 523, L2  
 Ackermann M. et al., 2010, *ApJ*, 721, 1383  
 Ackermann M. et al., 2012, *ApJ*, 747, 104  
 Ajello M. et al., 2009, *ApJ*, 699, 603  
 Angelakis E., Fuhrmann L., Marchili N., Krichbaum T. P., Zensus J. A., 2008, *Mem. Soc. Astron. Ital.*, 79, 1042  
 Anton S., Browne I. W. A., Marcha M. J., 2008, *A&A*, 490, 583  
 Arp H., Sargent W. L., Willis A. G., Oosterbaan C. E., 1979, *ApJ*, 230, 68  
 Atwood W. B. et al., 2009, *ApJ*, 697, 1071  
 Baars W. M., Zimmermann P., 1977, *A&A*, 61, 99  
 Barthelmy S. D. et al., 2005, *Space Sci. Rev.*, 120, 143  
 Baumgartner W. H., Tueller J., Markwardt C., Skinner G., 2010, *American Astron. Soc. HEAD Meeting*, 11, 13.05  
 Blandford R. D., 2000, *R. Soc. Lond. Philos. Trans. Series A*, 358, 811  
 Blandford R. D., Rees M. J., 1978, in Wolfe A. M., ed., *BL Lac Objects*. Univ. Pittsburgh Press, Pittsburgh, p. 328  
 Bollner T., Bradt W. N., Fink H., 1996, *A&A*, 305, 53  
 Bonnoli G., Ghisellini G., Foschini L., Tavecchio F., Ghirlanda G., 2011, *MNRAS*, 410, 648  
 Böttcher M., Dermer C. D., 2002, *ApJ*, 564, 86  
 Burrows D. N. et al., 2005, *Space Sci. Rev.*, 120, 165  
 Cardelli J. A., Clayton G. C., Mathis J. S., 1989, *ApJ*, 345, 245  
 Cash W., 1979, *ApJ*, 228, 939  
 Cusumano G. et al., 2010, *A&A*, 524, 64  
 Deo R. P., Crenshaw D. M., Kraemer S. B., 2006, *AJ*, 132, 321  
 Dermer C. D., Finke J. D., Krug H., Böttcher M., 2009, *ApJ*, 692, 32  
 Donato D., Perkins J. S., 2011, *Astron. Telegram*, 3452  
 Donato D., Sambruna R. M., Gliozzi M., 2005, *A&A*, 433, 1163  
 Finke J. D., 2012, *ApJ*, submitted  
 Finke J. D., Dermer C. D., Böttcher M., 2008, *ApJ*, 686, 181  
 Foschini L., 2011, *Proc. Conf. Narrow-Line Seyfert 1 Galaxies and Their Place in the Universe*, PoS 24, preprint (arXiv:1105.0772)  
 Foschini L., Maraschi L., Tavecchio F., Ghisellini G., Gliozzi M., Sambruna R. M., 2009, *Adv. Space Res.*, 43, 889  
 Foschini L. et al., 2011, *MNRAS*, 413, 1671  
 Fuhrmann L., Zensus J. A., Krichbaum T. P., Angelakis E., Readhead A. C. S., 2007, in Ritz S., Michelson P., Meegan C. A., eds, *AIP Conf. Proc. Vol. 921, The First GLAST Symposium*. Am. Inst. Phys., New York, p. 249  
 Fuhrmann L. et al., 2008, *A&A*, 490, 1019  
 Fuhrmann L. et al., 2011, *Proc. Conference Narrow-Line Seyfert 1 Galaxies and Their Place in the Universe*, PoS 26  
 Gehrels N. et al., 2004, *ApJ*, 611, 1005  
 Ghisellini G., Tavecchio F., 2008, *MNRAS*, 387, 1669  
 Ghisellini G., Tavecchio F., Foschini L., Ghirlanda G., 2011, *MNRAS*, 414, 2674  
 Giommi P. et al., 2012, *A&A*, 541, 160  
 Goodrich R. W., 1989, *ApJ*, 342, 224  
 Grandi P., 2011, *Proc. High Energy Phenomena in Relativistic Outflows III*, preprint (arXiv:1112.2505)  
 Grupe D. et al., 2010, *ApJS*, 187, 64  
 Jorstad S. G. et al., 2005, *AJ*, 130, 1418  
 Kalberla P. M. W., Burton W. B., Hartmann D., Arnal E. M., Bajaja E., Morris R., Pöppel W. G. L., 2005, *A&A*, 440, 775  
 Kataoka J. et al., 2011, *ApJ*, 740, 29  
 Komossa S., Allen A., McCray R., 2006, *AJ*, 132, 531  
 Konigl A., 1981, *ApJ*, 243, 700  
 Landau R. et al., 1986, *ApJ*, 308, 78  
 Lister M. et al., 2009, *AJ*, 137, 3718  
 Liu Y., Jiang D. R., Gu M. F., 2006, *ApJ*, 637, 669  
 Maoz D., Bahcall J. N., Doxsey R., Schneider D. P., Bahcall N. A., Lahav O., Yanny B., 1993, *ApJ*, 402, 69  
 Marscher A., 2009, in Belloni T., ed., *Lecture Notes in Physics*, Vol. 794, *Jets in Active Galactic Nuclei*. Springer, Berlin, p. 173  
 Marscher A. P., 2010, *ApJ*, 710, L126  
 Massaro E., Perri M., Giommi P., Nesci R., 2004, *A&A*, 413, 489  
 Mattox J. R. et al., 1996, *ApJ*, 461, 396  
 McLure R. J., Jarvis M. J., 2004, *MNRAS*, 353, L45  
 Meier D. L., 2003, *New Astron. Rev.*, 47, 667  
 Moore R. L., Stockman H. S., 1981, *ApJ*, 243, 60  
 Mor R., Netzer H., 2012, *MNRAS*, 240, 526  
 Nenkova M., Sirocky M. M., Nikutta R., Ivezić Ž., Elitzur M., 2008, *ApJ*, 685, 160  
 Nolan P. et al., 2012, *ApJS*, 199, 31  
 Nottale L., 1986, *A&A*, 157, 383  
 Orienti M., D'Ammando F., Giroletti M., 2012, *Fermi & Jansky Proc. – eConf. C111110*, preprint (arXiv:1205.0402)  
 Osterbrock D. E., Pogge R. W., 1985, *ApJ*, 297, 166  
 Pogge R. W., 2000, *New Astron. Rev.*, 44, 381

- Raiteri C. M. et al., 2010, *A&A*, 524, 43  
Raiteri C. M. et al., 2011, *A&A*, 534, 87  
Richards J. L. et al., 2011, *ApJS*, 194, 29  
Roming P. W. A. et al., 2005, *Space Sci. Rev.*, 120, 95  
Shen Y. et al., 2011, *ApJS*, 194, 45  
Sikora M., 2009, *Astron. Nachr.*, 330, 291  
Sikora M., Stawarz L., Lasota J.-P., 2007, *ApJ*, 658, 815  
Sitko M. L., Rudnick L., Jones T. W., Schmidt G. D., 1984, *PASP*, 96, 402  
Taylor G. et al., 2005, *ApJS*, 159, 27  
Vestergaard M., 2004, in Richards G. T., Hall P. B., eds, *ASP Conf. Ser.* Vol. 311, *AGN Physics with the Sloan Digital Sky Survey*. Astron. Soc. Pac., San Francisco, p. 69
- Wilms J., Allen A., McCray R., 2000, *ApJ*, 542, 914  
Yuan W., Zhou H. Y., Komossa S., Dong X. B., Wang T. G., Lu H. L., Bai J. M., 2008, *ApJ*, 685, 801  
Zhou H.-Y., Wang T.-G., Dong X.-B., Li C., Zhang X.-G., 2005, *Chin. J. Astron. Astrophys.*, 5, 41  
Zhou H.-Y. et al., 2006, *ApJS*, 166, 128  
Zhou H.-Y. et al., 2007, *ApJ*, 658, L13

This paper has been typeset from a  $\text{\TeX}/\text{\LaTeX}$  file prepared by the author.